EFFECT OF SURROUNDING GAS ON VELOCITY DISTRIBUTION FUNCTION OF MOLECULES IN MOLECULAR BEAM

A. E. Zarvin and R. G. Sharafutdinov

UDC 533.6.011

Molecular-beam methods have become widely used in recent times for the study of flows of rarefied gases [1]. However, the very first experiments with molecular beams for a gasdynamic source [2] showed that the measured intensities fell below theoretical predictions. Most devices for the creation of a molecular beam by means of a gasdynamic source have pumping equipment of comparatively low capacity and beam formation in them occurs with residual gas present. It was shown [3] that the residual gas penetrates into the jet and significantly reduces the intensity of the molecular beam. This and subsequent work [4, 5] were confined to measurements of intensity (density) and there are no data in the literature on the effect of residual gas on other parameters of the distribution function. The present work was devoted to a study of the effect of residual gas on the distribution function in a molecular beam defined from a jet in the scattering mode [6]. The work was performed on the small molecular-beam generator [7] and on the VS-4 low-density gasdynamic tube [8] at the Institute of Thermal Physics, Siberian Branch, Academy of Sciences of the USSR. Measurements of the distribution function by the time-of-flight method [9] were performed on the small molecular-beam generator and measurements of gas density on the VS-4.

The experiments on the small molecular-beam generator were performed in the following manner. A molecular beam was defined by means of a skimmer from a jet which was formed by escape of gas through a convergent nozzle. The beam was modulated in the post-skimmer chamber and passed through a collimator into the detection chamber where it was transformed into an electrical signal by an ionization detector. The signal from the detector was fed into a recording system for storage and averaging of information in order to increase the signal-to-noise ratio. Analysis of the data from time-of-flight measurements was performed by means of statistical regularization [10]. The density $n_{\parallel}$ of the molecular beam, the hydrodynamic velocity $w_{\parallel}$, and the parallel translational temperature $T_{\parallel}$ were calculated from the reconstructed distribution [11]. The error in the determination of these quantities did not exceed 10-15%. The technique for carrying out experiments on the VS-4 using an electron beam is described in [12, 13].

The experimental conditions are tabulated in Table 1, where Re_* is the Reynolds number calculated from the parameters in the critical section of the nozzle and from its diameter d_*; p_0 is the stagnation pressure; p_1 is the pressure of the residual gas in the expansion chamber; $N = p_0/p_1$ is the pressure ratio; $Re_L = Re_*/\sqrt{N}$; $S_{\parallel} = w_{\parallel}/\sqrt{2kT_{\parallel}/m}$ is the velocity ratio [14]; k is the Boltzmann constant; m is the mass of the gas; T_f is the limiting translational temperature; and T_0 is the stagnation temperature. Technically pure nitrogen with a stagnation temperature of approximately 290°K was used as the working gas.

The effect of the residual gas in the post-skimmer chamber on the parameters of the molecular beam was studied in the first set of experiments (see Table 1, modes 1-3). For this purpose, the pressure p_2 of the residual gas in the post-skimmer chamber was varied by throttling the evacuation system between the limits $2 \cdot 10^{-6}$ and $90 \cdot 10^{-6}$ mm Hg with fixed stagnation conditions and unchanged nozzle–skimmer distance. The pressure in the detection chamber remained roughly constant.

Figure 1a, b shows the molecular-beam density $n_{\parallel}$ and the velocity ratio $S_{\parallel}$ as functions of the pressure p_2 for two tabulated modes: 1 (curves 1 and 3) and 2 (curves 2 and 4). The values of $n_{\parallel}$ and $S_{\parallel}$ were

Novosibirsk. Translated from Zhurnal Prikladnoi Mekhaniki i Tekhnicheskoi Fiziki, No. 4, pp. 11-19, July-August, 1976. Original article submitted August 14, 1975.

TABLE 1

Mode	Re_*	p_0/p_1	Re_L	$S_{\parallel}$	T_f/T_0	Diagnostic method
1	155	3010	2,8	4,2	0,164	Time-of-flight
2	232	3000	4,2	4,7	0,138	»
3	282	2960	5,2	5,0	0,122	»
4	77	3000	1,4	3,5	0,225	»
5	154	2730	3,0	4,2	0,164	»
6	154	923	5,1	4,2	0,164	»
7	154	200	10,9	4,2	0,164	»
8	206	3200	3,6	4.5	0,144	»
9	206	1600	5,15	4,5	0,144	»
10	206	400	10,3	4,5	0,144	»
11	283	3140	5,1	5,0	0,121	»
12	283	880	9,6	5,0	0,121	»
13	283	366	14,8	5,0	0,121	»
14	153	2770	2,9	4,2	0,165	Electron beam
15	153	917	5,0	4,2	0,165	»
16	152	200	10,7	4,2	0,166	»
17	283	3150	5.0	5,0	0,122	»
18	283	863	9,7	5,0	0,122	»
19	283	360	15.0	5,0	0,122	»
20	3000	86 000	10.2	9.9	0,035	»

normalized to their maximum values n_m and S_m, which were obtained by extrapolating the data to $p_2 = 0$. An increase in the pressure of the residual gas in the post-skimmer chamber from $2 \cdot 10^{-6}$ to $\sim 60 \cdot 10^{-6}$ gives rise to a considerable drop in density (by roughly a factor of 2) for mode 2, while the velocity ratio shows no marked change. In this region, $\ln n_{\parallel}$ depends linearly on pressure. With further increases in p_2, there is observed a tendency toward a rise in density and a drop in the velocity ratio with the deviations from the initial behaviors for density and velocity ratio occurring almost simultaneously. Curves 1 and 3, which correspond to mode 1 with the smaller Reynolds number, show the same trend, but the effect of residual gas in the post-skimmer chamber on the parameters of the molecular beam becomes evident considerably sooner.

To understand the reasons for such behavior of the density and velocity-ratio curves, we consider what is recorded by a detector in the molecular beam. When the pressure of the residual gas is infinitely low, only molecules in the defined beam are incident on the detector. Gradual increase in pressure leads to scattering of these molecules and to an increase in the fraction of recorded background molecules. As long as the fraction of background molecules is small, the decrease in recorded density is exponential. Changes in hydrodynamic velocity and temperature are not observed, since the detector only sees those molecules which did not undergo collision or which were scattered at small angles on the path from the skimmer. Further increase in

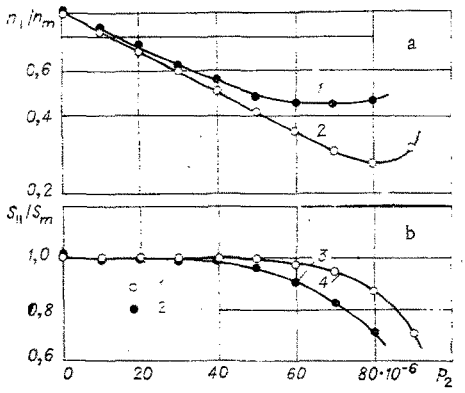

Fig. 1

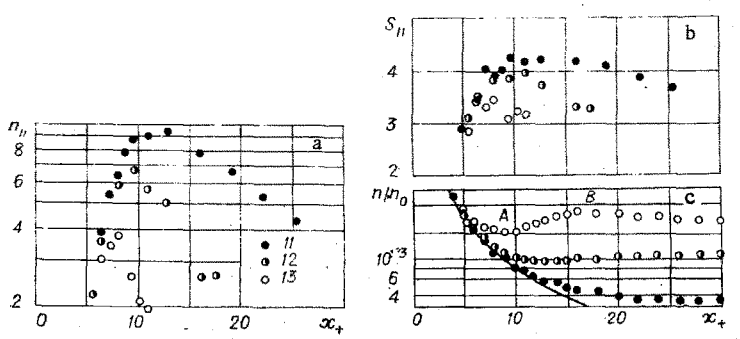

Fig. 2

p_2 leads to an increase in the contribution from molecules of the residual gas to the time-of-flight signal, which leads to a gradual broadening of the distribution function, to a decrease in the rate of fall of the density, and then to a rise that is proportional to the increase in p_2. Starting at some pressure, the detector will record mainly molecules of the residual gas from the post-skimmer chamber. Noticeable changes in the moments of the distribution function start at lower residual-gas pressures for modes with lower beam-particle densities at the entrance to the skimmer (curves 1 and 3 in Fig. 1).

The density dependence on the pressure p_2 (in the linear portion of Fig. 1a) can be described by means of the classical scattering formula

$$n_{\parallel}/n_m = \exp(-qn_2l_2), \tag{1}$$

where q is the differential scattering cross section; n_2 is the number density of residual-gas molecules in the post-skimmer chamber; and l_2 is the distance in which scattering occurs. One can find q from Eq. (1) by using the dependence of $n_{||}/n_m$ on p_2 (see Fig. 1a) and by assuming the distance l_2 is equal to the linear dimension of the post-skimmer chamber. The nitrogen–nitrogen differential scattering cross section calculated in this way was found to be approximately $110 \cdot 10^{-16}$ cm^2, which is consistent with the results of other authors.

A second set of measurements was devoted to a study of the effect of residual gas in the expansion chamber on the recorded parameters of the molecular beam. The measurements were made over the following parameter ranges: Re_*, from 75 to 300; p_0/p_1, from 200 to 3000; Re_L, from 1.4 to 15; the measurements were carried out on the small molecular-beam generator and on the VS-4 (see Table 1, modes 4-13 and modes 14-20, respectively). Typical examples of the changes in the molecular-beam density $n_{||}$ (in arbitrary units) and in the velocity ratio $S_{||}$ as a function of the nozzle–skimmer distance in units of nozzle-tip diameter, $x_+ = x/d_*$, are shown in Fig. 2a, b. The measurements were made under constant stagnation conditions and varying pressures of the residual gas. Scattering in the post-skimmer chamber was taken into account in the analysis of the results. The rise in the density and velocity-ratio curves in the initial portion (at small x_+) was caused by gradual opening of the skimmer because of an increase in the Knudsen number of the skimmer. The skimming effect does not depend on the pressure in the surrounding space. In the absence of other causes having an effect on beam parameters, therefore, measurements of $n_{||}$ and $S_{||}$ for all p_1 should fall on a single curve. Such a coincidence occurs only at small x_+ within the limits of experimental error. As x_+ increases, the departure from a common curve occurs earlier when p_1 is higher. Further, the density and velocity ratio pass through a maximum and decrease with subsequent increase in x_+. Such behavior of $n_{||}$ and $S_{||}$ was also noted for other modes. The density and velocity ratio also decrease when there is an increase in the pressure of the surrounding space at a fixed distance from the nozzle. Since a study of skimmer interaction is not the subject of this paper, all the results in the following will be given only for distances x_+ downstream from the maxima of $n_{||}$ and $S_{||}$ where the skimmer interaction can obviously be neglected (for the three modes shown in Fig. 2, the Knudsen numbers calculated from the local mean free path in the skimmer cutoff and from the diameter of the cutoff evaulated at the maxima of the curves in Fig. 2a are 3.5, 2.25, and 1.3 for modes 11, 12, and 13, respectively; for the other modes (4-10) the Knudsen numbers are higher than those given).

Figure 2c shows measurements of the density n on the axis of the jet normalized to the stagnation density n_0 for the same conditions as in the case of Fig. 2a, b. Calculated results for isentropic flow at $\gamma = 1.4$ (γ is the ratio of heat capacities) are shown by the solid line. In regions close to the nozzle, the density in the jet agrees with calculated values and it is equal to the density in the surrounding space in regions removed from the nozzle. While the density curve shows a rise from point A to point B when $Re_L \simeq 15$, which corresponds

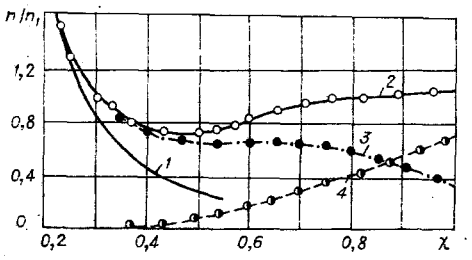

Fig. 3

to the structure of a diffuse Mach disk, such a rise is completely absent from $Re_L \simeq 5$ and a smooth transition occurs to a density equal to the density of the surrounding space.

Figure 3 shows the distribution of the partial densities of the components on the axis of an N_2 jet escaping into a CO atmosphere (mode 20), which was obtained by means of an electron beam in earlier studies [15]. The measured partial density relative to the background density, n/n_1, is plotted on the ordinate and the reduced coordinate $\chi = x_+/\sqrt{N}$ is plotted along the abscissa. Curve 1 is an isentropic calculation; curves 2-4 are, respectively, the total density, the density of the gas in the jet, and the density of the penetrating component from the surrounding space. According to Fig. 3, the deviation of the gas density in the jet from the isentropic calculation takes place in a region where the presence of molecules of the penetrating component cannot yet be recorded.

The results shown in Figs. 2 and 3 were obtained with jets which are in the scattering mode. In this mode, gas molecules having a directed velocity collide with molecules penetrating into the jet from the surrounding space. These collisions lead to the appearance of scattered molecules of the gas in the jet. If the gas in the surrounding space has the same composition as the gas in the jet, (which happens in most cases except for specially formulated experiments [6, 15]), the molecules of the surrounding space and the scattered molecules from the jet are indistinguishable. These two types form a gas background in which scattering of molecules with a directed velocity in the jet occurs. As is clear from Fig. 2c, the density of this background is almost constant and is considerably higher than the density of the unscattered molecules.

Both unscattered molecules from the jet and background molecules are incident on the molecular-beam detector. The number of background molecules reaching the detector can be estimated from formulas for an effusion source with a temperature and pressure equal to that in the surrounding space and with an opening having a diameter equal to the diameter of the skimmer cutoff. The molecular-beam density for efflux into a vacuum and $S_{||} \geq 3$ is given by [14]

$$n_\infty \simeq n \frac{r^2}{L^2}\left(S_{||}^2 + \frac{1}{2}\right)\left(\frac{x}{x_f}\right)^2, \tag{2}$$

where n is the gas density in the cutoff of a skimmer of radius r; L is the skimmer–detector distance. This expression was obtained for the case where the last-collision surface is upstream of the skimmer. According to [16], the density on the axis of the jet has the form

$$\frac{n}{n_0} = B\frac{1}{x_+^2}, \tag{3}$$

where $B \simeq 0.089$ for $\gamma = 1.4$. An estimate of x_f can be made from the value of the limiting Mach number M_f [14] assuming that the flow is continuous and is described by isentropic relations for $\gamma = 1.4$ up to M_f. In that case,

$$x_f/d_* \sim (p_0 d_*/T_0)^{1/2}.$$

The dependence of the limiting Mach number on the ratio of heat capacities in the form given in [14] was only experimentally confirmed for argon but the dependence of x_f/d_* on the parameters p_0, d_*, and T_0 obviously is also maintained for other gases. Therefore,

$$x_f/d_* \sim (p_0 d_*/T_0)^\alpha. \tag{4}$$

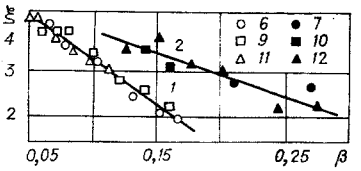

Fig. 4

The choice of α is made in accordance with measurements. Upon substitution of Eqs. (3) and (4) into Eq. (2) we obtain

$$n_\infty \simeq \frac{B}{k}\frac{r^2}{L^2}\left(\frac{p_0}{T_0}\right)^{1-2\alpha} d_*^{-2\alpha}\left(S_\parallel^2+\frac{1}{2}\right). \tag{5}$$

This expression indicates that the density in the molecular beam is constant and its level is determined by stagnation parameters downstream from the last-collision surface. The number of molecules with directed velocity at the detector in the molecular beam, as calculated from Eq. (5), is two to three orders of magnitude greater than the number of background molecules reaching the detector over almost the entire region of measurement.

Scattering in the expansion chamber can be considered in the same way as in the post-skimmer chamber:

$$n_\parallel = n_{--}e^{-q_1 n_1 (x_1 - x_-)}, \tag{6}$$

where q_1 is the differential scattering cross section determined from the kind of gases in the jet and in the surrounding space and from the solid angle of the skimmer–detector system; x_1 is the distance from the nozzle tip along the axis of the jet; x_- is the coordinate of the beginning of the scattering region with a constant background density; n_- is the density in the molecular beam at a nozzle–skimmer distance equal to x_-. In accordance with Fig. 2c, the density of background molecules can be assumed equal to the density n_1 of the gas in the surrounding space. The validity of the use of such a scattering law for molecules reaching the detector was first demonstrated in [3]. In the present work, as in [3], the quantity $\ln n_\parallel$ depends linearly on the coordinate. Results obtained at large values of the normalized coordinate $\chi > 0.6$ are an exception. In this region, the contribution to the measured signal from background molecules becomes comparable to that made by molecules having a directed velocity. The density n_- and the coordinate x_- are not determined in Eq. (6). Their indeterminacy is associated with the fact that there is no sharp boundary between efflux into a vacuum and into a scattering region with a constant density of scattering particles; it is assumed $n_- \simeq n_\infty$. The question of the value of x_- will be discussed below.

According to [6], the parameter $R = d_* \sqrt{p_0 p_1}/T_0$ is a similarity criterion for the penetration process in the scattering mode. In [17], an analogous criterion, Re_L, was proposed for generalization of the penetration process. At constant T_0, $Re_L \sim d_* \sqrt{p_0 p_1}$, i.e., it agrees with the parameter R to the order of a constant factor. The similarity criteria R and Re_L are the inverse of the Knudsen number σ based on the length of the mean free path in the surrounding space and the maximum dimension of the jet evaluated in accordance with [16].

It was shown [17] that the profiles of the density of the gas in the jet and the density of the penetrating component are generalized in terms of the similarity coordinates $(n/n_0)B/\sqrt{N} \sim \chi$ for constant Re_L. Much the same similarity can be expected for the density in the molecular beam. Indeed, the results shown in Fig. 4 for the measured density $n_\parallel$ in the scattering mode expressed in terms of the variables ξ and β, where $\xi = \ln [n_\parallel p_0^{2\alpha-1}/(S_\parallel^2 + 1/2)]$ and $\beta = x_+ p_1$, fall on a single straight line when Re_L = const. Parameters which remain constant in the experiments are omitted. From the similarity of the scattering process (Fig. 4) follows the fact that the product $x_- p_1$ is unchanged when Re_L is fixed and that neglecting it can only give an additive displacement of the origin along the x axis, which is unimportant for the present discussion.

The exponent α was taken to be 0.4. Here, as in the following graphs, the data shown correspond to regions of decrease in density and velocity ratio as x_+ increases (Fig. 2a, b), i.e., to conditions where skimmer interaction has little effect.

As is clear from Fig. 4, the slope of the lines is determined by Re_L. The smaller Re_L, the steeper the slope is and the more intense the scattering. One can assume that the scattering intensity is inversely proportional to Re_L. The density in the molecular beam then is

$$n_\parallel \simeq \frac{B}{k}\frac{r^2}{L^2}\left(\frac{p_0}{T_0}\right)^{1-2\alpha} d_*^{-2\alpha}\left(S_\parallel^2+\frac{1}{2}\right) e^{-\frac{q_1 n_1 (x_1 - x_-)}{Re_L}}.$$

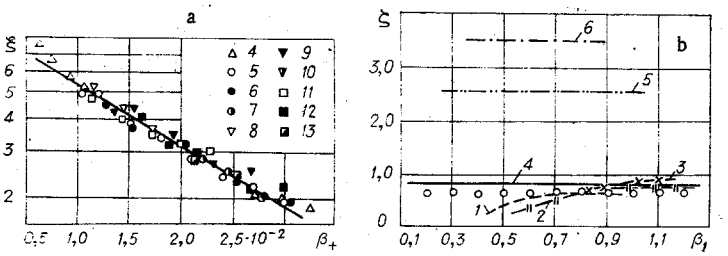

Fig. 5

In this case, the dependence of ξ on $\beta_+ = \beta/Re_L$ should be constant for all Re_L. This conclusion is nicely confirmed by Fig. 5a where measurements at various Re_L are shown. It should be noted that this generalization is possible in the range of Re_L corresponding to the region of applicability of the condition requiring constant density of the molecules in the scattering gas. This condition breaks down when $Re_L > 10$–15 [15].

A comparison of the experimental data with other results [3, 5] is presented in Fig. 5b. The measurements of density (or intensity) in the papers being compared were presented in arbitrary units and therefore the only comparison possible is that of the slopes of the relations for the density of the molecular beam during scattering in terms of generalized coordinates. For this purpose, the slopes of the curves compared, $\zeta = d \cdot (\ln \xi)/d\beta_1$, are plotted along the ordinate and $\beta_1 = q_1 n_1 x_1/Re_L$ is plotted along the abscissa. At the present time, the authors do not have publications available where measurements of the velocity distribution function in the molecular beam for various p_0 and p_1 were given together with the density. In plotting the experimental data in [3, 5], in generalized coordinates, therefore, the assumption was made that the velocity ratio was constant for all x_+ and equal to its limiting value S_f calculated in accordance with [13]. The conversion of the measured molecular-beam intensity in these papers to density was made by means of the expression $n = I/w_f$, where w_f is the hydrodynamic velocity determined at the freezing point. The differential scattering cross section for nitrogen was assumed to be $110 \cdot 10^{-16}$ cm^2 and that for argon, $149 \cdot 10^{-16}$ cm^2 [5].

As is clear from Fig. 5b, good agreement of the data (shown by the points) was obtained with the results of [5] for argon (curve 1, $p_1 = 2.26$ mm Hg; curve 2, $p_1 = 4.52$ mm Hg; curve 3, $p_1 = 6.8$ mm Hg). Some increase in ζ as β_1 increases for maximum p_1 is obviously connected with the failure to consider the change in velocity ratio. On the other hand, the condition for constant density of the scattering molecules is not fulfilled at lower pressures of the residual gas even at large distances from the nozzle tip. The density of the scattering gas decreases upstream with a resultant drop in the effectiveness of the process and a corresponding decrease in the slopes of the curves. The absence of generalization of the experimental data in [3] for nitrogen (curve 4, $p_0 = 10$ mm Hg; curve 5, $p_0 = 50$ mm Hg; curve 6, $p_0 = 100$ mm Hg) may result from the effect of molecules reflected from the rear wall of the skimmer and from the variation in velocity ratio not taken into consideration in the comparison.

The effect of scattering on the distribution function is illustrated in Fig. 2b where the variation of the velocity ratio is shown as a function of the nozzle–skimmer distance for three modes with varying pressures in the surrounding space. The decrease in velocity ratio with increasing x_+ may be associated, first, with an increase in the number of molecules incident on the detector after collision with the background gas, and, second, with an increase in the relative fraction of the molecules of the surrounding space recorded by the detector. The second effect should also lead to a change in the behavior of the density dependence on distance in the direction of a relative increase of the density above an exponentially decreasing curve. Such a relative increase in density was actually noted at large distances from the nozzle tip. However, this effect was insignificant over the greater portion of the range of x_+. Under these conditions, according to Fig. 5a, the variation of the density of a molecular beam with scattering taken into consideration is proportional to the variation of $S^2_{||}$.

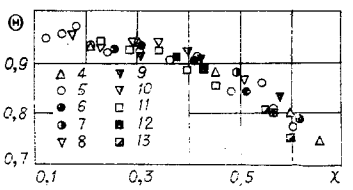

Fig. 6

Figure 6 shows the generalization of the experimental data for temperature in the modes 4-13. The combination $\Theta = (T_{||} - T_0)/(T_f - T_0)$ is plotted on the ordinate and the distance in reduced coordinates is plotted on the abscissa. All the data fall on a single curve within the limits of experimental error. Data related to the region of strong skimmer interaction do not generalize in terms of the reduced coordinates and are not shown here. As is clear from Fig. 6, all points fall below unity, i.e., the temperature in the molecular beam nowhere reaches its limiting value (calculated from S_f).

The authors are grateful to A. K. Rebrov for valuable discussions.

LITERATURE CITED

1. T. A. Milne and F. T. Greene, "Molecular beams in high-temperature chemistry," in: Advances in High-Temperature Chemistry, Vol. 2, Academic Press, New York (1969).
2. E. W. Becker and K. Bier, "Die Erzeugung eines intensiven, teilweise monochromatisierten Wasserstoff-Molekularstrahles mit einer Laval-Düse," Z. Naturforsch., 9a, No. 11 (1954).
3. J. B. Fenn and J. B. Anderson, "Background and sampling effects in free jet studies by molecular-beam measurements," in: Rarefied Gas Dynamics, Fourth International Symposium, Vol. 2, Academic Press, New York (1966).
4. R. F. Brown and J. H. Heald, Jr., "Background gas scattering and skimmer interaction studies using a cryogenically pumped molecular-beam generator," in: Rarefied Gas Dynamics, Fifth International Symposium, Vol. 2, Academic Press, New York (1967).
5. T. R. Govers, R. L. LeRoy, and J. M. Deckers, "The concurrent effects of skimmer interactions and background scattering on the intensity of a supersonic molecular beam," in: Rarefied Gas Dynamics, Sixth International Symposium, Vol. 2, Academic Press, New York (1969).
6. E. P. Muntz, B. B. Hamel, and V. L. Maguire, "Exhaust plume rarefaction," AIAA Paper 69-657 (1969).
7. A. E. Zarvin, "Use of a molecular beam to study low-density flows," in: Experimental Methods in Dynamics of Rarefied Gases [in Russian], Izd. Inst. Teplofiz. Sibirsk. Otd. Akad. Nauk SSSR, Novosibirsk (1974).
8. A. A. Bochkarev, E. G. Velikanov, A. K. Rebrov, R. G. Sharafutdinov, and V. N. Yarygin, "Gasdynamic installations of low density," in: Experimental Methods in Dynamics of Rarefied Gases [in Russian], Izd. Inst. Teplofiz. Sibirsk. Otd. Akad. Nauk SSSR, Novosibirsk (1974).
9. O. F. Hagena and A. K. Varma, "Time-of-flight velocity analysis of atomic and molecular beams," Rev. Sci. Instr., 39, No. 1 (1968).
10. Yu. E. Voskoboinikov and Ya. Ya. Tomson, "Reconstruction of the execution of input signal in measuring systems," in: Electrodiffusion Diagnostics for Turbulent Flows [in Russian], Izd. Inst. Teplofiz. Sibirsk. Otd. Akad. Nauk SSSR, Novosibirsk (1973).
11. D. R. Willis and B. B. Hamel, "Nonequilibrium effects in spherical expansions of polyatomic gases and gas mixtures," in: Rarefied Gas Dynamics, Fifth International Symposium, Vol. 1, Academic Press, New York (1967).
12. A. A. Bochkarev, V. A. Kosinov, A. K. Rebrov, and R. G. Sharafutdinov, "Measurement of gas-flow parameters by means of an electron beam," in: Experimental Methods in Dynamics of Rarefied Gases [in Russian], Izd. Inst. Teplofiz. Sibirsk. Otd. Akad. Nauk SSSR, Novosibirsk (1974).
13. V. A. Kosinov, L. P. Kuznetsov, and R. G. Sharafutdinov, "Experimental technique in electron-beam diagnostics," in: Experimental Methods in Dynamics of Rarefied Gases [in Russian], Izd. Inst. Teplofiz. Sibirsk. Otd. Akad. Nauk SSSR, Novosibirsk (1974).
14. J. B. Anderson and J. B. Fenn, "Velocity distribution in molecular beams from nozzle sources," Phys. Fluids, 8, No. 5 (1965).
15. N. I. Kislyakov, A. K. Rebrov, and R. G. Sharafutdinov, "Diffusion processes in the mixing region of a supersonic low-density jet," Zh. Prikl. Mekh. Tekh. Fiz., No. 1 (1973).
16. H. Ashkenas and F. S. Sherman, "The structure and utilization of supersonic free jets in low-density wind tunnels," in: Rarefied Gas Dynamics, Fourth International Symposium, Vol. 2, Academic Press, New York (1966).
17. V. V. Volchkov, A. V. Ivanov, N. I. Kislyakov, A. K. Rebrov, V. A. Sukhnev, and R. G. Sharafutdinov, "Low-density jets outside an acoustic nozzle at high-pressure drops," Zh. Prikl. Mekh. Tekh. Fiz., No. 2 (1973).